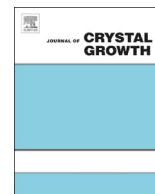




ELSEVIER

Contents lists available at ScienceDirect

Journal of Crystal Growth

journal homepage: [www.elsevier.com/locate/jcrysgr](http://www.elsevier.com/locate/jcrysgr)

# Multi-GPUs parallel computation of dendrite growth in forced convection using the phase-field-lattice Boltzmann model

Shinji Sakane<sup>a</sup>, Tomohiro Takaki<sup>b,\*</sup>, Roberto Rojas<sup>c</sup>, Munekazu Ohno<sup>d</sup>, Yasushi Shibuta<sup>e</sup>, Takashi Shimokawabe<sup>f</sup>, Takayuki Aoki<sup>f</sup>

<sup>a</sup> Graduate School of Science and Technology, Kyoto Institute of Technology, Matsugasaki, Sakyo-ku, Kyoto 606-8585, Japan

<sup>b</sup> Faculty of Mechanical Engineering, Kyoto Institute of Technology, Matsugasaki, Sakyo-ku, Kyoto 606-8585, Japan

<sup>c</sup> Department of Mechanical Engineering, Escuela Politécnica Nacional, Ladrón de Guevara E11-253, 17-01-2759 Quito, Ecuador

<sup>d</sup> Division of Materials Science and Engineering, Faculty of Engineering, Hokkaido University, Kita 13 Nishi 8, Kita-ku, Sapporo, Hokkaido 060-8628, Japan

<sup>e</sup> Department of Materials Engineering, The University of Tokyo, 7-3-1 Hongo, Bunkyo-ku, Tokyo 113-8656, Japan

<sup>f</sup> Global Scientific Information and Computing Center, Tokyo Institute of Technology, 2-12-1 i7-3 i7-3 O-okayama, Meguro-ku, Tokyo 152-8550, Japan

## ARTICLE INFO

Communicated by Dr Francois Dupret

Keywords:

- A1. Computer simulation
- A1. Dendrites
- A1. Convection
- A1. Crystal morphology

## ABSTRACT

Melt flow drastically changes dendrite morphology during the solidification of pure metals and alloys. Numerical simulation of dendrite growth in the presence of the melt flow is crucial for the accurate prediction and control of the solidification microstructure. However, accurate simulations are difficult because of the large computational costs required. In this study, we develop a parallel computational scheme using multiple graphics processing units (GPUs) for a very large-scale three-dimensional phase-field-lattice Boltzmann simulation. In the model, a quantitative phase field model, which can accurately simulate the dendrite growth of a dilute binary alloy, and a lattice Boltzmann model to simulate the melt flow are coupled to simulate the dendrite growth in the melt flow. By performing very large-scale simulations using the developed scheme, we demonstrate the applicability of multi-GPUs parallel computation to the systematical large-scale-simulations of dendrite growth with the melt flow.

## 1. Introduction

Dendrites are typical morphological structures in the solidification of pure metals and alloys. Dendrite solidification structures are largely affected by the melt convection [1–3]. Owing to the recent development of in situ X-ray imaging techniques, many solidification phenomena caused by or affected by the melt flow, such as dendrite fragmentation [4,5] and freckle formation [6,7], have been revealed. However, for a deep understanding of such multi-physics problems, it is important to investigate the phenomena by means of not only in situ X-ray observations but also computer simulations that can simulate dendrite growth in the melt flow. In addition, the in situ observations are currently performed for thin samples. Therefore, it is especially important to develop a numerical scheme for predicting the solidification conditions in three-dimensional (3D) bulk crystals.

The cellular automaton (CA) method has been widely used to simulate dendrite growth in melt flows such as forced convection [8,9] and natural convection [10,11] flows. Recently, very-large-scale simulations have been reported by coupling CA with the lattice Boltzmann method (LBM) [12,13]. The CA method is a powerful tool for

simulating the interaction of multiple dendrites in a relatively wide computational domain. However, the accuracy required to express dendrite morphology is sacrificed in CA simulations for multiple dendrites. The phase-field (PF) method has recently emerged as a powerful numerical model for expressing dendrite morphology with high accuracy [14–16]. The PF method has also been applied to dendrite growth problems under melt flow [17,18]. However, most of the PF simulations reported so far have focused on two-dimensional (2D) domains [19–29], and 3D PF simulations have only been carried out in only a few studies [30–32]. In 3D PF simulations of dendrite growth under melt flow, the adaptive mesh refinement (AMR) scheme was employed. The AMR scheme is a very powerful scheme used for reducing the computational cost in PF simulations. This is because the PF simulation requires fine meshes only around the interface region [33–36]. However, the programming of AMR is generally complicated, and its computational efficiency becomes poor when the volume fraction of the interface is large [37].

Recently, graphics processing units (GPUs) have been used for general-purpose computations, i.e., GPGPU. The GPGPU has made acceleration of the computation of a wide variety of applications

\* Corresponding author.

E-mail address: [takaki@kit.ac.jp](mailto:takaki@kit.ac.jp) (T. Takaki).

<http://dx.doi.org/10.1016/j.jcrysgr.2016.11.103>

Available online xxxx

0022-0248/ © 2016 Elsevier B.V. All rights reserved.

possible, including problems in computational materials science [38–45]. We have developed a parallel GPU computation to accelerate a very-large-scale phase-field simulation of the directional solidification of a binary alloy and showed that parallel GPU computation is well suited for phase-field simulations [46–48]. In particular, we have successfully achieved a very-large-scale 3D phase-field simulation of the directional solidification of a binary alloy polycrystal in a system with dimensions of  $3.072 \times 3.078 \times 3.072 \text{ mm}^3$  ( $4096 \times 4104 \times 4096$  meshes) for a total simulation time of more than 100 s (4 million computational steps) using 768 GPUs on the supercomputer TSUBAME2.0 [47]. It is the largest simulation of dendrite growth currently reported, to the best of our knowledge. We have also applied a quantitative phase-field model [49] to the parallel GPU computation and investigated the competitive dendrite growth during directional solidification [50–53].

In this study, we develop a parallel GPU computational scheme, which systematically and efficiently enables large-scale simulations of dendrite growth under the melt flow by coupling PF and LBM by utilizing the state-of-art technique of parallel GPU computation. First, we extend the 2D phase-field-lattice Boltzmann model (PFLBM) [54,55] to the 3D case for simulating dendrite growth in the presence of melt flow, and then we develop parallel GPU code to accelerate the large-scale 3D PFLBM simulation. Finally, large-scale simulations of dendrite growth in forced convection are performed using TSUBAME2.5, the GPU-rich supercomputer at the Tokyo Institute of Technology.

## 2. Phase-field-lattice Boltzmann model

In this work, the phase-field-lattice Boltzmann model (PFLBM) developed by Rojas et al. [54] is extended to the 3D case. In PFLBM, the quantitative phase-field model for the dendrite growth of a dilute binary alloy [49] and the lattice Boltzmann model for the melt flow [56] are coupled. Here, the translational and rotational motion of the dendrite is ignored for the sake of simplicity; however, the PFLBM developed by Rojas et al. [54] can describe the motion of the dendrite. The phase-field method is the only way to simulate the dendrite growth accurately [57], and our quantitative model can provide the correct results independently on the interface thickness. The lattice Boltzmann model is easy to implement and is also easy to be parallelized comparing to directly solving the Navier-Stokes equations. Namely, the PFLBM is very powerful for the high accurate parallel GPU simulation of dendrite growth with melt flow.

### 2.1. Quantitative phase-field model for dilute binary alloy solidification

The phase-field  $\phi$  is defined as  $\phi = +1$  in solid and  $\phi = -1$  in liquid. In dimensionless time and distance normalized by relaxation time  $\tau_0$  and the interface thickness parameter  $W_0$ , respectively, the evolution equation of  $\phi$  is expressed by

$$a_s^2 \frac{\partial \phi}{\partial t} = \nabla [a_s^2 \nabla \phi] + \frac{\partial}{\partial x} \left[ a_s \frac{\partial a_s}{\partial \phi_x} |\nabla \phi|^2 \right] + \frac{\partial}{\partial y} \left[ a_s \frac{\partial a_s}{\partial \phi_y} |\nabla \phi|^2 \right] + \frac{\partial}{\partial z} \left[ a_s \frac{\partial a_s}{\partial \phi_z} |\nabla \phi|^2 \right] - f'(\phi) - \lambda^* g'(\phi) u. \quad (1)$$

Here,  $a_s$  is an interface anisotropy function given by

$$a_s(\tilde{\nabla} \phi) = (1 - 3\zeta) \left[ 1 + \frac{4\zeta}{1 - 3\zeta} \frac{\phi_{\tilde{x}}^4 + \phi_{\tilde{y}}^4 + \phi_{\tilde{z}}^4}{|\tilde{\nabla} \phi|^4} \right]. \quad (2)$$

where  $\zeta$  is the strength of anisotropy and  $(\tilde{x}, \tilde{y}, \tilde{z})$  is a material coordinate system that corresponds to the  $\langle 100 \rangle$  direction. The differentiation of  $\phi$  with respect to  $(\tilde{x}, \tilde{y}, \tilde{z})$ ,  $\tilde{\nabla} \phi$ , is obtained by the following coordinate transformation using the Euler angles  $(\varphi, \theta, \psi)$  in

rotation sequence  $x$ - $y$ - $x$ :

$$\begin{aligned} \begin{pmatrix} \frac{\partial \phi}{\partial \tilde{x}} \\ \frac{\partial \phi}{\partial \tilde{y}} \\ \frac{\partial \phi}{\partial \tilde{z}} \end{pmatrix} &= \begin{bmatrix} \frac{\partial x}{\partial \tilde{x}} & \frac{\partial y}{\partial \tilde{x}} & \frac{\partial z}{\partial \tilde{x}} \\ \frac{\partial x}{\partial \tilde{y}} & \frac{\partial y}{\partial \tilde{y}} & \frac{\partial z}{\partial \tilde{y}} \\ \frac{\partial x}{\partial \tilde{z}} & \frac{\partial y}{\partial \tilde{z}} & \frac{\partial z}{\partial \tilde{z}} \end{bmatrix} \begin{pmatrix} \frac{\partial \phi}{\partial x} \\ \frac{\partial \phi}{\partial y} \\ \frac{\partial \phi}{\partial z} \end{pmatrix} = \begin{bmatrix} 1 & 0 & 0 \\ 0 & \cos \psi & \sin \psi \\ 0 & -\sin \psi & \cos \psi \end{bmatrix} \begin{bmatrix} \cos \theta & 0 & -\sin \theta \\ 0 & 1 & 0 \\ \sin \theta & 0 & \cos \theta \end{bmatrix} \\ &= \begin{bmatrix} 1 & 0 & 0 \\ 0 & \cos \varphi & \sin \varphi \\ 0 & -\sin \varphi & \cos \varphi \end{bmatrix} \begin{pmatrix} \frac{\partial \phi}{\partial x} \\ \frac{\partial \phi}{\partial y} \\ \frac{\partial \phi}{\partial z} \end{pmatrix}. \end{aligned} \quad (3)$$

Here, we rotate first about the  $x$ -axis by an angle  $\varphi$ , then the  $y$ -axis by an angle  $\theta$ , and finally the  $x$ -axis by an angle  $\psi$ . In Eq. (1),  $f'(\phi) = -\phi + \phi^3$  and  $g'(\phi) = (1 - \phi)^2$  are the first derivative functions of the double-well potential and the interpolating function of chemical free energy of each phase, respectively. The dimensionless concentration  $u$  is defined by

$$u = \frac{C_l - C_l^e}{C_l^e - C_s^e}. \quad (4)$$

where  $C_l$  is the solute concentration in liquid, and  $C_l^e$  and  $C_s^e$  are the equilibrium solute concentrations in liquid and solid, respectively. By following the Kim–Kim–Suzuki (KKS) model [58], we use the relations  $k = C_s/C_l = C_s^e/C_l^e$  and  $C = \phi C_s + (1 - \phi) C_l$ , where  $k$  is the partition coefficient and  $C$  is the solute concentration. Moreover,  $\lambda^* = a_1 W_0/d_0$  is a constant related to the thermodynamical driving force, where  $a_1 = 0.88388$  [16] and  $d_0$  is the chemical capillary length defined by

$$d_0 = \frac{\Gamma}{|m|(1 - k)c_l^e}, \quad (5)$$

where  $\Gamma$  is the Gibbs-Thomson coefficient and  $m$  is the liquidus slope.

The time evolution of the dimensionless solute concentration  $u$  is expressed by

$$\frac{[1 + k - (1 - k)\phi]}{2} \left( \frac{\partial u}{\partial t} + \mathbf{U} \cdot \nabla u \right) = \nabla (D_l q(\phi) \nabla u - j_{AT}) + \frac{[1 + (1 - k)u]}{2} \frac{\partial \phi}{\partial t} - \nabla \cdot \mathbf{J}. \quad (6)$$

where  $\mathbf{U}$  is the melt flow velocity, and  $D_l$  and  $D_s$  are the diffusivities in the liquid and solid, respectively. Besides,  $j_{AT}$  is the anti-trapping current expressed by

$$j_{AT} = -a(\phi) W_0 [1 + (1 - k)u] \frac{\partial \phi}{\partial t} \frac{\nabla \phi}{|\nabla \phi|}, \quad (7)$$

where  $q(\phi) = (kD_s + D_l + (kD_s - D_l)\phi)/2D_l$  is the interpolating function. To initiate higher-order branching in the dendrite,  $\nabla \cdot \mathbf{J}$  is introduced as a noise term [59]. The relaxation time  $\tau_0$  is expressed as  $\tau_0 = a_2 \lambda^* W_0^2 / D_l$  with  $a_2 = 0.6267$  [16]. Eqs. (1) and (6) are discretized by the finite difference method. The time differentiations are discretized by the first-order forward difference method. Isotropic discretization [60] using the nearest and next-to-nearest neighbor grid points and the second-order central difference approximation are used for the Laplace operator of Eq. (1) and Eq. (7), respectively. For the computation of the advection term in Eq. (6), the weighted essentially non-oscillatory (WENO) fifth-order scheme is used.

### 2.2. Lattice Boltzmann model

In the following formulation of the lattice Boltzmann equation, we use dimensionless time and distance normalized by the time increment  $\Delta t$  and the lattice size  $\Delta x$ , respectively. The lattice Boltzmann equation that considers an external force term is expressed by

Download English Version:

<https://daneshyari.com/en/article/5489237>

Download Persian Version:

<https://daneshyari.com/article/5489237>

[Daneshyari.com](https://daneshyari.com)